Fuel Processing Technology 172 (2018) 29–35

Contents lists available at ScienceDirect

Fuel Processing Technology

journal homepage: www.elsevier.com/locate/fuproc

Hydrodeoxygenation and hydroisomerization of palmitic acid over bi-functional Co/H-ZSM-22 catalysts

Yaya Cao[a,1], Yanchun Shi[b,1], Yunfei Bi[e], Kejing Wu[b], Shaojian Hu[b], Yulong Wu[b,c,*], Shaobin Huang[a,d]

[a] College of Environment and Energy, South China University of Technology, Guangzhou 510006, PR China
[b] Institute of Nuclear and New Energy Technology, Tsinghua University, Beijing 100084, PR China
[c] Beijing Engineering Research Center for Biofuels, Beijing 100084, PR China
[d] Guangdong Provincial Key Laboratory of Atmospheric Environment and Pollution Control, Guangzhou 510006, PR China
[e] Laboratory of Hydrogenation, Research Institute of Petroleum Processing, Sinopec, Beijing 100083, China

ARTICLE INFO

Keywords:
Hydrodeoxygenation
Hydroisomerization
Palmitic acid
Co/H-ZSM-22

ABSTRACT

Hydrodeoxygenation and hydroisomerization of palmitic acid were achieved over bi-functional Co/H-ZSM-22 catalysts (about 4 wt% Co loading), and the maximum of isoproducts reached up to 73.4% selectivity at 260 °C for 4 h in presence of 2 MPa H_2. Compared to parent H-ZSM-22, the impregnation of Co species for bi-functional catalysts could catalyze completely palmitic acid conversion into 100% selectivity of alkanes in spite of low pressure (1 MPa H_2). Furthermore, bi-functional Co/H-ZSM-22 catalysts tailored the deoxygenation route via hydrodeoxygenation leading to more C_{16} formation. With decreasing of reaction pressure, mole ratio of C_{16}/C_{15} decreased during complete conversion of palmitic acid, indicating that low reaction pressure favored hydrodecarbonylation to produce more C_{15}. Bi-functional Co/H-ZSM-22 catalysts also exhibited great stability after five runs without any deactivation.

1. Introduction

The increasing jet fuel demand, petroleum fuel depletion and the greenhouse effect, have widely motivated great attention in developing bio-based jet fuel [1]. Compared with the traditional petroleum-based jet fuel, bio-based jet fuel can dramatically decrease CO_2 emitting from fuels life cycle from 55 to 90%. As well known, quality jet fuel possesses low freezing point, which is required to meet highly stringent international standards, such as lower than − 55 °C for civilian and − 60 °C for military. The ideal composition of jet fuel was C_9–C_{16} iso-alkanes and cycloalkanes. Among the biomass feedstock, fatty acids (C_8–C_{18}) account for microalgae-based bio-oil up to 60%, and stearic acid (C_{18})/palmitic acid (C_{16}) are usually regarded as the model compounds to investigate the deoxygenation for bio-oil [2]. Based upon appropriate carbon numbers, upgrading of microalgae oil to bio-based jet fuel is considered as one of the most potential way, which has attracted extensive attention all over the world. There are many publications reporting on bio-diesel production from microalgae based bio-oil [3–7]. However, some disadvantages of microalgae based bio-oil, such as low heating value, corrosiveness, thermal instability, high viscosity, have hindered its use in practice because of high oxygen content, up to 35–40%. Therefore, deoxygenation is the key to upgrading of microalgae based bio-oil [8].

So far, there are three deoxygenation methods of bio-oil reported as follows: hydrodexygenation (HDO) [9,10], hydrodecarbonylation (HDC), [11] and decarboxylation (DCX) [12]. Considering carbon atom economy, HDO is the most promising deoxygenation method without losing the carbon atom. In our previous works, MoO_2/CNTs and Co-doped MoO_2/CNTs catalysts have been developed to upgrading of palmitic acid, and *n*-C_{16} was obtained as main products [13,14]. Despite of the suitable carbon numbers, the freezing point is too high for jet fuel because of *n*-alkanes products. For example, the freezing point of *n*-C_{16} is 20 °C, but the freezing point of *7,8*-dimethyl-C_{14} (*multi.*iso-C_{16}) is − 70 °C. Therefore, isomerization of *n*-alkanes is necessary for producing bio-based jet fuel. Zeolite supports have been extensively studied in various industrial fields including catalysts for isomerization and cracking of long chain alkanes over their acid sites (Brönsted and Lewis acid sites, especially for Brönsted acid sites) [15,16]. Recently, bi-functional metal/zeolite catalysts have been developed to upgrading of bio-oil. For example, Peng et al. investigated that upgrading of palmitic

* Corresponding author at: Institute of Nuclear and New Energy Technology, Tsinghua University, Beijing 100084, PR China.
E-mail address: wylong@tsinghua.edu.cn (Y. Wu).
[1] The first two authors contributed equally to this work.

https://doi.org/10.1016/j.fuproc.2017.09.020
Received 4 June 2017; Received in revised form 29 August 2017; Accepted 19 September 2017
0378-3820/ © 2017 Published by Elsevier B.V.

acid over Ni/ZrO_2 [17], Ni/H-beta (Si/Al = 75, 5 wt% Ni loading) and Ni/H-ZSM-5 (Si/Al = 45, 10 wt% Ni loading) [18], and found that all *n*-alkanes over Ni/ZrO_2, 18.8% and 6.7% selectivity of iso-alkanes over Ni/H-beta and Ni/H-ZSM-5, respectively. Zhao et al. [19] also reported that it obtained 11% selectivity of isoproducts during stearic acid conversion over Ni/H-beta catalysts (31% Ni loading,Si/Al = 11). Cheng et al. [1] optimized reaction conditions to improve bio-based jet fuel quality over Ni-Mo/HY catalyst (8 wt% Ni loading and 12 wt% Mo loading) and yielded 48.2% jet fuel in presence of 1 MPa H_2. In our previous researches, HDO and isomerization could be simultaneously achieved by the Mo/ZSM-22 [20] and Ni/HZSM-22 [21] catalysts during upgrading of bio-oil. 59.7% selectivity of iso-C_{16} were observed over Mo/H-ZSM-22 catalyst at 260 °C for 4 h in the presence of 4 MPa H_2, and strong acid sites were beneficial for isomerization. As for Ni/H-ZSM-22 catalyst with melt infiltration, there were 16.5% selectivity of iso-C_{15} and 28.8% selectivity of iso-C_{16} with complete conversion of palmitic acid at 260 °C for 4 h in presence of 4 MPa H_2, respectively. High temperature was proven to favor the formation of iso-products. It can be seen that the combination of the metal centers and acid sites over bi-functional metal/zeolite catalysts would catalyze palmitic acid with high activity to produce iso-alkanes.

In this work, palmitic acid and H-ZSM-22 with high excellent isomerization, were selected as the model compound of microalgae derived bio-oil and acid-support. Metal Co is reported to possess excellent hydrogenation function [5–7,22–24], thus it is intentionally selected as metal centers. Moreover, an efficient and appropriate preparation method for bi-functional metal/zeolite catalysts usually influences on their physicochemical properties and final catalytic performance, especially for deoxygenation routes and selectivity of final products. In our previous work [21], bi-functional Ni/H-ZSM-22 catalysts with incipient wetness impregnation and melt infiltration methods, exhibited more excellent catalytic performance. However, it was a pity that there was no obvious difference in deoxygenated routes and selectivity of final products over Ni/H-ZSM-22 catalysts with different preparation methods. From this view, bi-functional Co/H-ZSM-22 catalysts were prepared by these two methods to evaluate the deoxygenation routes and acid-catalyzed performance of palmitic acid in this paper. The aims of this study are to compare with the differences and commons of physicochemical properties and catalytic performance under the different H_2 pressures through the above two methods, especially to get more iso-alkanes with low freezing point. Meanwhile, the characterization methods, including XRD, TEM, XRF, XPS, N_2 adsorption-desorptionanalysis, H_2-TPR and NH_3-TPD, were used to systematically analyze the interaction between metal centers and acid sites over bi-functional Co/H-ZSM-22 catalysts, and their synergistic effect on catalytic performance. Finally, compared to Ni/H-ZSM-22, there would be discussed the influence of Co on hydrodeoxygenation and final product distribution over bi-functional Co/H-ZSM-22 catalysts during bio-oil upgrading.

2. Experiments

2.1. Catalysts preparation

The catalysts Co particles supported onto H-ZSM-22 zeolites (Si/Al = 37.5) were prepared by incipient wetness impregnation and melt infiltration methods with same CoO loading (5.0 wt%). The synthesized procedures were described as following: the quantities of aqueous Co$(NO_3)_2{\cdot}6H_2O$ were dissolved in an amount of various distilled water, and then slowly dropped this solution onto calcined zeolitic supports H-ZSM-22 with continuous stirring. After impregnating the metal precursor on the supports for 4 h at ambient temperature, prepared by incipient wetness impregnation sample was oven dried at 105 °C overnight. As for the catalyst using the melt infiltration method, Co$(NO_3)_2{\cdot}6H_2O$ and support H-ZSM-22 were mixed uniformly in a closed vial, and then dried at 65 °C for 24 h. The obtained two methods prepared Co/H-ZSM-22 catalysts were calcined in air atmosphere at 550 °C with a heating rate of 2 °C·min^{-1}, and then maintained the set temperature for 6 h. The two calcined catalysts were reduced at 500 °C for 4 h (heating ramp: 10 °C·min^{-1}) in a constant H_2 flow (flow rate: 80 mL·min^{-1}). For convenience, the reduced catalysts were defined as Co/HZ-n, which Co/HZ-1 represented the catalyst using the incipient wetness impregnation method and Co/HZ-2 using melt infiltration method, respectively.

2.2. Catalysts characterization

Powder X-ray diffraction (XRD) were used to evaluate the phase structures of the obtained catalysts. The diffraction patterns were recorded on a D/MAX-III X-ray diffractometer (Rigaku Corporation, Japan) with filtered Cu K α radiation at a tube current of 35 mA and a voltage of 35 kV, which data were collected on the scanning 2θ range of 5–80°. The relative crystallinity of catalysts was calculated by the sum of the peak intensities at 2θ of 8.1, 10.1, 12.7, 20.3, 24.3, and 25.7°, and the crystallinity of parent HZ-22 was defined as 100%. Transmission electron microscopy (TEM) images taken with a Model FEI Quanta were used to examine the surface morphologies and particle sizes of Co/HZ-n catalysts. The elemental analyses of the solids were obtained by X-ray fluorescence (XRF) spectrometer MagiX (Philips). X-Ray photoelectron spectroscopy (XPS) measurements were performed on a PHI5300 X-ray photoelectron spectrometer with a monochromatic X-ray source (Al Kα), which used to detect the atom content on the zeolites surface. Nitrogen adsorption-desorption isotherms on a Micromeritics ASAP 2010 instrument was used to examine the specific surface area analysis of the Co/HZ-n catalysts. The total surface area of Co/HZ-n was calculated by application of the Brunauer-Emmett-Teller (BET) equation, using the relative pressure ranging from 0.05 to 0.16 in the nitrogen adsorption isotherm with the linear range (using a molecular cross-sectional area for 0.162 nm^2 N_2). The samples were first handled outgassed under vacuum at 363 K for 1 h, and then at 623 K for 15 h. The micropore volume was calculated by the t-plot method. The acidity (amount and strength) of H-type zeolites and reduced Co/HZ-n catalysts was measured by Temperature-programmed desorption of ammonia (NH_3-TPD), which was carried out on an Autochem II 2920 unit with a thermal conductivity detector (TCD). Co/HZ-n catalysts were characterized by H_2temperatureprogrammedreduction (H_2-TPR, a TP-5076 multiple adsorption instrument), which was performed from room temperature up to 500 °C with 10 °C·min^{-1} in a flow of 5% H_2/N_2. The consumption of H_2 was also analyzed online equipped with a thermal conductivity detector.

2.3. Catalytic HDO tests

Catalytic reactions for upgrading of palmitic acid were carried out in a stainless autoclave with 150 mL batch mode. Atypical reaction was performed as follows: palmitic acid (0.5 g), catalyst (0.1 g), *n*-decane (50 mL). At the beginning of reaction, the above dissolved solution was injected into the autoclave, and then purged with the H_2 at ambient temperature for three times, and then the H_2 pressure regulated to 4, 2 and 1 MPa. The mixture was heated from room temperature to reaction temperature (260 °C) for 4 h under constant stirring (300 rpm).The final liquid phase products were analyzed by an Agilent GC–MS (7890–597-5) using a FSFS J &W 122–5532 (30 m × 250 μm × 0.25 μm) column and a flame ionization detector (FID). Conversion of palmitic acid and selectivity of products were calculated as follows:

$$\text{Coversion of palmitic acid} = \frac{\text{moles of converted palmitic aicd}}{\text{mole of the strating palmitic aicd}} \times 100\%; \quad (1)$$

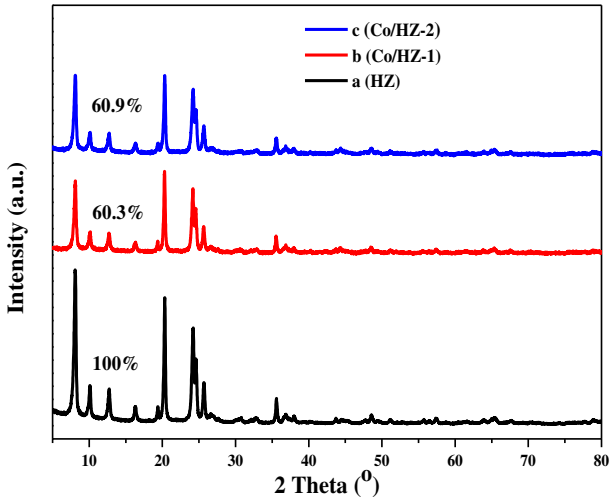

Fig. 1. XRD patterns of calcined parent zeolites HZ (a) and reduced Co/HZ-n catalysts (b: the incipient wetness impregnation method; c: melt infiltration method).

$$\text{Selectivity of products} = \frac{\text{moles of each product}}{\text{moles of total products}} \times 100\% \quad (2)$$

3. Results and discussion

3.1. Physicochemical properties of catalysts

Fig. 1 shows the XRD patterns of calcined parent zeolites HZ (Fig. 1a) and reduced Co/HZ-n using the incipient wetness impregnation method (Fig. 1b, Co/HZ-1) and using melt infiltration method (Fig. 1c, Co/HZ-2).The all characteristic peaks for all samples were similar with the parent zeolites HZ, and no additional diffraction peaks of other zeolites competed phases were detected by XRD. The relative crystallinity of reduced Co/HZ-1 (Fig. 1b, samples prepared by incipient wetness impregnation method) and Co/HZ-2 (Fig. 1c, samples prepared by melt infiltration method) decreased up to 60.3% and 60.9%, respectively, compared to parent HZ (crystallinity defined as 100%). The obvious decrease of crystallinity for reduced Co/HZ-n catalysts may be ascribed to two reasons: (i) the zeolite structure destructed to some extent during calcination and reduction; (ii) the much massive attenuation coefficient of Co atoms [25]. No obvious diffraction peaks of Co^0 or CoO_x were detected for reduced Co/HZ-n catalysts, probably because of low Co loading (4 wt% in this paper) and/or well dispersion of Co^0 over parent HZ [26]. Fig. 2 shows TEM images of calcined parent HZ (Fig. 2a), reduced Co/HZ-1 (Fig. 2b, incipient wetness impregnation method) and Co/HZ-2 (Fig. 2c, melt infiltration method) catalysts. Like the case of parent HZ, Co/HZ-n catalysts exhibited similar needle-like shape crystals. Meanwhile, size of Co particles over Co/HZ-1 (20–50 nm) was larger than that over Co/HZ-2 (about 20 nm), disclosing that melt infiltration method may be beneficial for Co particles dispersed over zeolitic supports to form smaller particles.

Co/Si mole ratios of reduced Co/HZ-1 (incipient wetness impregnation method) and Co/HZ-2 (melt infiltration method) were detected by XRF and XPS analysis as presented in Table 1. Co/HZ-1 possessed slight higher Co/Si (0.043 by XRF and 0.013 by XPS) than Co/HZ-2 (0.041 by XRF and 0.011 by XPS). Compared to XRF results, XPS analysis results indicated that most of Co particles could enter into pores of support ZSM-22. Table 2 shows the textural properties of parent supports (HZ) and reduced Co/HZ-n catalysts by XRF and N_2 adsorption-desorption analysis. According to XRF analysis, the impregnation of Co did not influence the Si/Al ratios (mol/mol) of parent HZ at 37.5, and Co loading of Co/HZ-1 and Co/HZ-2 were 3.9 wt% and 3.7 wt%, respectively. Compared with parent HZ, S_{BET} of reduced Co/

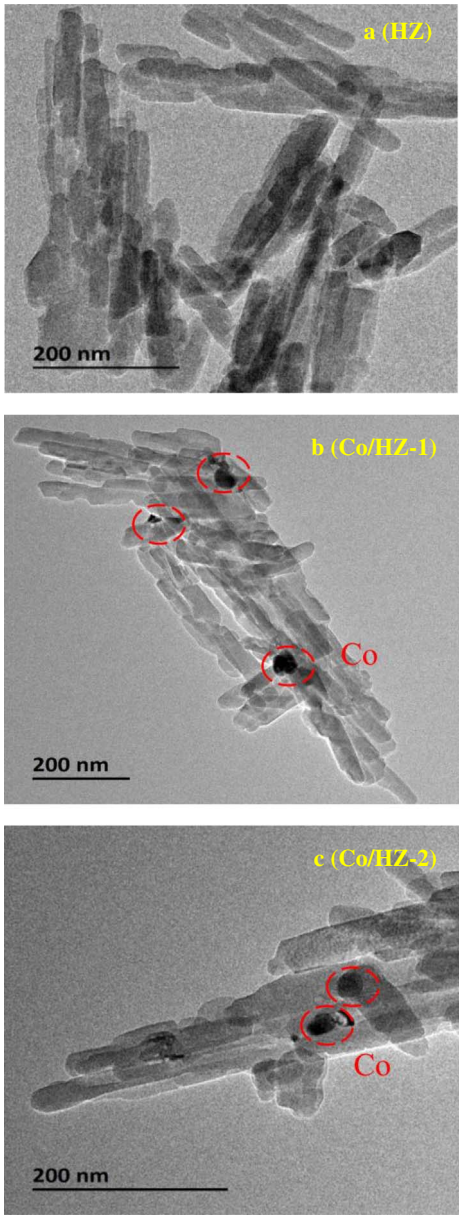

Fig. 2. TEM images of calcined parent zeolites HZ (a) and reduced Co/HZ-n catalysts (b: the incipient wetness impregnation method; c: melt infiltration method).

Table 1
Co/Si mole ratio of reduced Co/HZ-n with incipient wetness impregnation and melt infiltration methods.

Catalysts	Co/Si mole ratio (XRF)	Co/Si mole ratio (XPS)
Co/HZ-1	0.043	0.013
Co/HZ-2	0.041	0.011

Table 2
Textural properties of HZ and reduced Co/HZ-n with incipient wetness impregnation and melt infiltration methods.

Catalysts	Si/Al (mol/mol)	Co loading (wt%)	S_{BET} (m^2/g)	S_{micro} (m^2/g)	V_{micro} (cm^3/g)	V_{total} (cm^3/g)
HZ	37.5	–	204	161	0.08	0.31
Co/HZ-1	37.5	3.9	144	107	0.05	0.30
Co/HZ-2	37.5	3.7	131	94	0.04	0.31

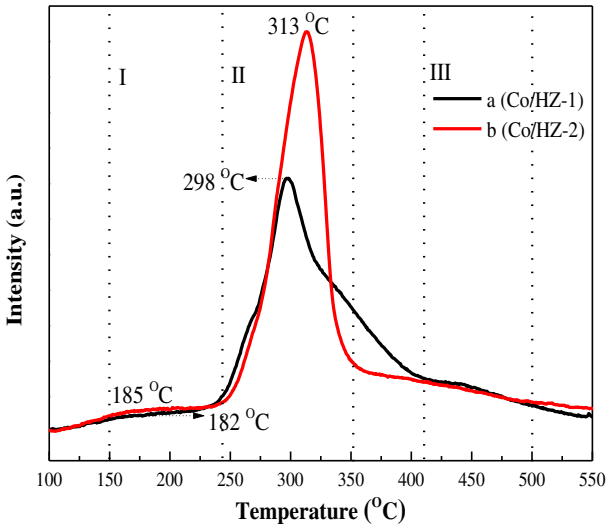

Fig. 3. H_2-TPR curves of calcined Co/HZ-n catalysts (a: the incipient wetness impregnation method; b: melt infiltration method).

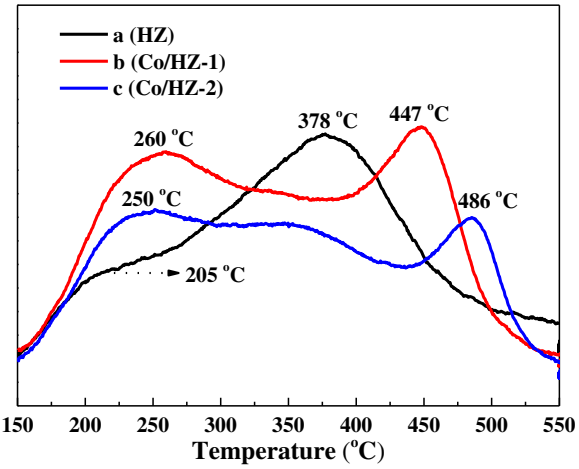

Fig. 4. NH_3-TPD curves of calcined parent zeolites HZ (a) and reduced Co/HZ-n catalysts (b: the incipient wetness impregnation method; c: melt infiltration method).

HZ-n samples decreased from 204 m^2/g (HZ) to 144 m^2/g (Co/HZ-1), 131 m^2/g (Co/HZ-2) after Co impregnation, so did S_{micro} (decreased from 161 m^2/g of HZ to 107 m^2/g of Co/HZ-1, 94 m^2/g of Co/HZ-2) and V_{micro} (decreased from 0.08 cm^3/g of HZ to 0.05 cm^3/g of Co/HZ-1, 0.04 cm^3/g of Co/HZ-2). These results indicated that there were some blockage occurred in the micro pores channels by Co^0 particles, which was good agreement with the TEM analysis results. Additionally, Co/HZ-2 presented more serious blockage of micropores than Co/HZ-1, suggesting that melt infiltration method was more beneficial to Co particles entered into zeolitic micropores.

3.2. Active centers of catalysts

3.2.1. Metal active centers

Fig. 3 shows the reducibility of calcined Co/HZ-n catalysts by the H_2-TPR measurement. There were three peaks of Co/HZ-n catalysts at approximately 150–240 °C ($Co_3O_4 \rightarrow CoO$), 240–350 °C ($CoO \rightarrow Co$), and 410–500 °C (strong interaction between metal and zeolite) [2]. As the XRD results shown, cobalt oxides were completely reduced to metal cobalt by H_2 at 500 °C for 4 h. Compared to Co/HZ-1 (182 and 298 °C), Co/HZ-2 possessed higher reduction temperatures (185 and 313 °C), indicating more Co particles located on zeolitic micropores by melt infiltration method [27,28]. This result was consistent with BET analysis with more serious blockage of Co/HZ-2 micropores. Meanwhile, the dominating H_2 consumption peak (313 °C) of calcined Co/HZ-2 was symmetrical, also implying that Co^0 particles well-dispersed over parent HZ with uniform accommodation. Different preparation methods of Co/HZ-n catalysts resulted in different location of Co particles over H-ZSM-22 supports, even leading to different deoxygenation routes.

3.2.2. Acid centers

The acidic properties of calcined parent zeolites HZ and reduced Co/HZ-n catalysts are shown in Fig. 4 detected by NH_3-TPD. There were two peaks of parent HZ around 205 and 378 °C (Fig. 4a), which were assigned to weak acid sites and strong acid sites, respectively. The impregnation of Co significantly enhanced the acid strength and amount of acid sites in Co/HZ-1 (260 and 447 °C in Fig. 4b) and Co/HZ-2 (250 and 486 °C in Fig. 4c), probably because of new acid sites formation [29]. Generally Co has weak acidity, and the metal introduced into zeolitic supports usually exhibits two effects of acidity based upon introduction of Co: the coverage of zeolitic acid sites and the formation of new acid sites on the zeolitic surface [30,31]. Obviously there were two effects over reduced Co/HZ-n catalysts. On one hand, the decrease of temperature peaks area around 378 °C indicated the coverage of originated acid sites possessed by zeolite micorpores. On the other hand, the higher temperatures were observed over Co/HZ-1 (260 and 447 °C in Fig. 4b) and Co/HZ-2 (250 and 486 °C in Fig. 4c), implying that the introduction of Co significantly improved the amount of weak acid sites and strong acid sites, even new strong acid sites produced. In addition, Co/HZ-1 presented more weak and strong acid sites than Co/HZ-2, probably due to its slightly higher Co content (3.9 wt% Co loading for Co/HZ-1; 3.7 wt% Co loading for Co/HZ-2). Co/HZ-1 (incipient wetness impregnation method) seemed less amount of Co particles entered into zeolitic pores than Co/HZ-2 (melt infiltration method) based upon BET analysis, which suggested that there was less coverage of zeolitic acid sites leading to expose more acid sites over Co/HZ-1 catalyst.

Generally for metal/support catalysts, supports are contributed to the dispersion and decrease of metal particles, which lead to enhance their activity, selectivity and catalyst life during deoxygenation of bio-oil/model compounds. During conversion of palmitic acid, the deoxygenation and C atom arrangement were both achieved over acid zeolitic supports. However, there was few literatures to report that the location (internal pores or external surface) of metal particles over zeolites affect deoxygenation routes of palmitic acid and selectivity of final products. In our previous work [21], more C_{16} (major) alkanes with some isoproducts were produced over Ni/H-ZSM-22 catalysts than that (C_{15} alkanes as major products) of single zeolites and Ni-oxide supports (SiO_2, Al_2O_3, ZrO_2 and so on) [17]. Based upon above characterizations in this paper, Co particles partially located in ZSM-22 pores with well-dispersion, and the impregnation Co particles enhanced acid sites and strength, obviously different from Ni/H-ZSM-22 [21]. These results may tailor deoxygenation routes of palmitic acid and selectivity of final products to some extent. Additionally, Co particles themselves may exhibit different catalytic performance, compared to Ni particles.

3.3. Catalytic performances over Co/HZ-n catalysts

3.3.1. Influence of different H_2 pressure

The upgrading of palmitic acid for the deoxygenation and isomerization were explored over reduced Co/HZ-n catalysts at 260 °C for 4 h in presence of 4 MPa H_2. As Fig. 5A and Table 3 (4 MPa H_2) shown, besides 6.3 wt% C_{15}-COOH detected over parent HZ, the main products distributed in *n*-C_{16}, isoC_{16}, *n*-C_{15}, isoC_{15}, and a slight cracking of *n*-C_{14}. Table 3 (4 MPa H_2) shows the corresponding selectivity of *n*-C_{16}, iso-C_{16}, *n*-C_{15}, iso-C_{15} and *n*-C_{14}. Clearly, the impregnation of Co over bi-

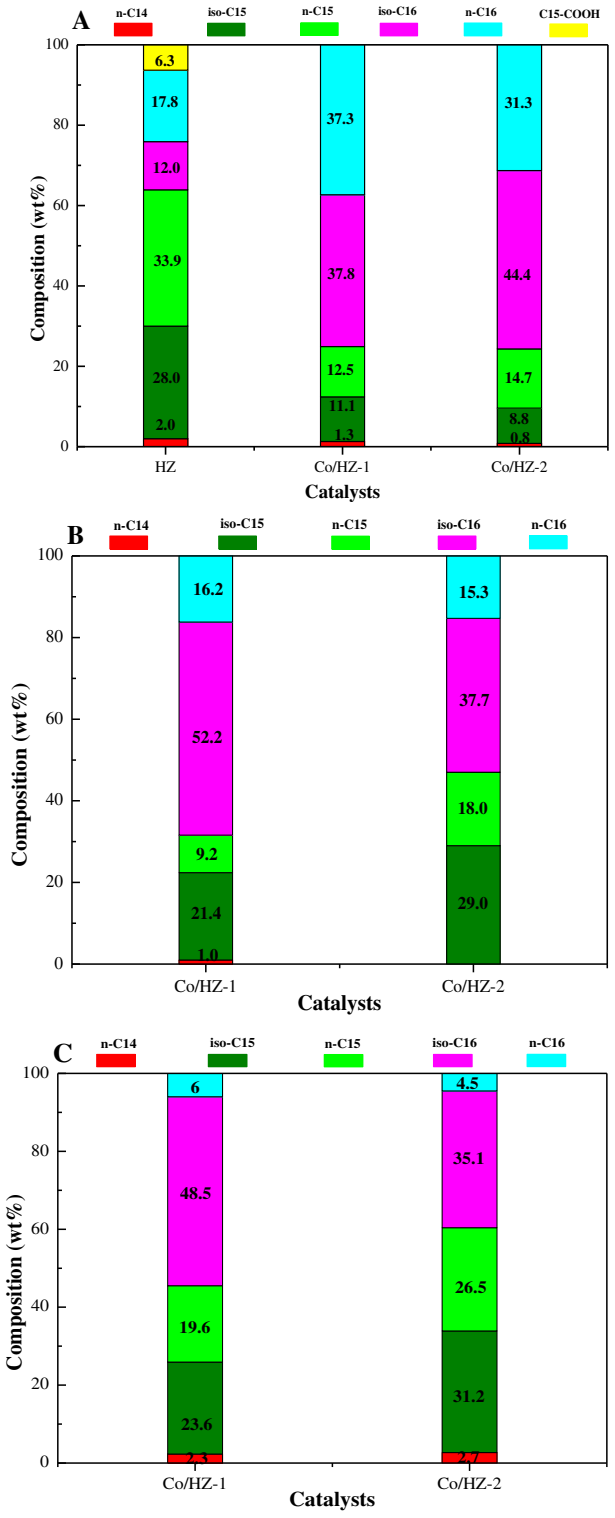

Fig. 5. Product compositions of palmitic acid over reduced Co/HZ-n catalysts at different hydrogen pressures (general conditions: 50 mL *n*-decane, 0.5 g palmitic acid, 0.1 g reduced Co/HZ-n catalysts, 260 °C, 4 h reaction time, stirring at 300 rpm).
A: 4 MPa H_2 B: 2 MPa H_2 C: 1 MPa H_2.

functional Co/HZ-n catalysts simultaneously enhanced the activity of palmitic acid conversion and selectivity of iso-products (48.8% for Co/HZ-1 and 52.9% for Co/HZ-2), compared to parent HZ (42.6% iso-products) showing that strong acid sites favored more iso-alkanes formation. There was main C_{15} production (36.9% *n*-C_{15} and 30.4% iso-C_{15}) over parent HZ, indicating the deoxygenation of palmitic acid mainly via HDC route. On the contrary, more *n*-C_{16} (36.7% for Co/HZ-1 and 30.8% for Co/HZ-2) and iso-C16 (37.2% for Co/HZ-1 and 43.6% for Co/HZ-2) were observed over bi-functional Co/HZ-n catalysts, which suggested that the impregnation of Co could change the deoxygenation of palmitic acid mainly via HDO route. However, there were similar iso-alkanes/*n*-alkanes (1.0 for Co/HZ-1 and 1.1 for Co/HZ-2) and C_{16}/C_{15} (both 3.0 for two bi-functional Co/HZ-n catalysts) mole ratios over bi-functional Co/HZ-n catalysts in presence of 4 MPa H_2, implying no significant differences in catalytic performances over Co/HZ-n prepared by incipient wetness impregnation and melt infiltration methods.

Based upon the above results, Co/HZ-1 and Co/HZ-2 exhibited similar catalytic performances of palmitic acid upgrading in presence of 4 MPa H_2 with high activity and selectivity of iso-products. When the pressure decreasing up to 2 MPa H_2, complete conversion of palmitic acid and 100% selectivity of alkanes were also obtained over bi-functional Co/HZ-1 (incipient wetness impregnation) and Co/HZ-2 (melt infiltration method) catalysts to show high activity. As shown in Fig. 5B, the main products were *n*-C_{16}, isoC_{16}, *n*-C_{15}, isoC_{15}, and a slight cracking of *n*-C_{14}. The corresponding selectivity of products are presented in Table 3 (2 MPa H_2). Compared to the results in presence of 4 MPa H_2, there was obvious difference in selectivity of products between Co/HZ-1 and Co/HZ-2 in presence of 2 MPa H_2. Co/HZ-1 yielded more C_{16} products with higher C_{16}/C_{15} mole ratio (2.1) and more iso-products with higher iso-alkanes/*n*-alkanes (2.8) than Co/HZ-2 (1.1 for C_{16}/C_{15} and 2.0 for iso-alkanes/*n*-alkanes). There might be two reasons [1]: Co/HZ-1 contained more Co loading than Co/HZ-2 by XRF and XPS analysis in Table 1 and Table 2. The higher Co loading, the more metal centers. Co centers favored HDO route of palmitic acid deoxygenation. Therefore, higher Co loading led to more C_{16} formation [2]. Co/HZ-1 showed more weak and strong acid sites than Co/HZ-2, which indicated that more isoproducts were formed over Co/HZ-1 catalyst [20,21]. Moreover, Co/HZ-2 showed stronger acidity than Co/HZ-1 by NH_3-TPD in Fig. 4, resulting in more C_{15} production via HDC route [20,21].

In presence of 1 MPa H_2, bi-functional Co/HZ-1 and Co/HZ-2 catalysts amazedly yielded 100% selectivity of alkanes with complete deoxygenation of palmitic acid (Fig. 5C and Table 3 1 MPa), showing excellent catalytic performance. The main products were similar to the results of high pressures. High isoalkanes/*n*-alkanes (2.5) and C_{16}/C_{15} (1.3) were obtained over Co/HZ-1, compared to those of Co/HZ-2 (1.9 isoalkanes/*n*-alkanes and 0.7 C_{16}/C_{15}). It is worth to note that C_{16} decreased with the decrease of pressure, indicating low pressure favored HDC route leading to more C_{15} formation. From the above results, it could be concluded that 2 MPa H_2 was more suitable to get much higher selectivity of isoalkanes (73.4% for Co/HZ-1, 66.6% for Co/HZ-2) and less cracking products regardless of the decrease of C_{16}/C_{15} ratio. More branched alkanes could meet the demand of lower freezing point of jet fuel.

3.3.2. Compared Co/HZ-1 to Ni/HZ-2 catalysts with identical preparation method (incipient wetness impregnation method)

In our previous work [21], the selectivity of main products over Ni/HZ-2 (incipient wetness impregnation method, for example) was 0.8% of *n*-C_{14}, 17.4% of iso-C_{15}, 26.4% of *n*-C_{15}, 24.2% of iso-C_{16} and 31.2% of *n*-C_{16} with complete conversion of palmitic acid at 260 °C for 4 h in presence of 4 MPa H_2. For this paper under identical reaction conditions (260 °C, 4 h, 4 MPa H_2), the selectivity of main products over Co/HZ-1 (incipient wetness impregnation method) was 1.4% of *n*-C_{14}, 11.6% of iso-C_{15}, 13.1% of *n*-C_{15}, 37.2% of iso-C_{16} and 36.7% of *n*-C_{16} with complete conversion of palmitic acid as well. It can be seen that Co/HZ-1 yielded more mole ratios of both iso-alkanes/*n*-alkanes (1.0) and C_{16}/C_{15} (3.0) than Ni/HZ-2 (0.7 of iso-alkanes/*n*-alkanes and 1.3 of C_{16}/C_{15}) with same preparation (incipient wetness impregnation method). On the one hand, Co particles seem to favor HDO route to form more C_{16} products, compared to Ni particles over identical zeolitic support H-ZSM-22. On the other hand, the impregnation of Co particles

Table 3
Conversion (%) and product selectivity (%) of palmitic acid over HZ and reduced Co/HZ-n catalysts.

H_2 pressure (MPa)	Catalysts	Conv. (%)	Selectivity (%)					Iso-alkanes/*n*-alkanes (mol/mol)	C_{16}/C_{15} (mol/mol)
			n-C_{14}	Iso-C_{15}	*n*-C_{15}	Iso-C_{16}	*n*-C_{16}		
4	HZ	93.7	2.3	30.5	36.8	12.2	18.2	–	–
	Co/HZ-1	> 99	1.4	11.6	13.1	37.2	36.7	1.0	3.0
	Co/HZ-2	> 99	0.9	9.3	15.4	43.6	30.8	1.1	3.0
2	Co/HZ-1	> 99	1.2	22.3	9.6	51.1	15.8	2.8	2.1
	Co/HZ-2	> 99	–	30.0	18.6	36.6	14.8	2.0	1.1
1	Co/HZ-1	> 99	2.5	24.4	20.3	47.0	5.8	2.5	1.3
	Co/HZ-2	> 99	3.0	31.9	27.1	33.7	4.3	1.9	0.7

Table 4
Time (h) of bi-functional Co/HZ-1 catalyst in upgrading of palmitic acid at 260 °C for 4 h in presence of 2 MPa H_2.

Catalysts	Time (h)	Conv. (%)	Selectivity (%)					Iso-alkanes/*n*-alkanes (mol/mol)	C_{16}/C_{15} (mol/mol)
			n-C_{14}	Iso-C_{15}	*n*-C_{15}	Iso-C_{16}	*n*-C_{16}		
Co/HZ-1	0.5	> 99	0.4	12.1	16.8	42.1	28.6	1.2	2.2
	1	> 99	0.6	10.7	18.4	45.3	25.0	1.3	2.1
	2	> 99	0.9	16.1	12.6	48.9	21.5	1.8	2.1
	4	> 99	1.2	22.3	9.6	51.1	15.8	2.8	2.1

Table 5
Recycles of bi-functional Co/HZ-1 catalyst in upgrading of palmitic acid at 260 °C for 4 h in presence of 2 MPa H_2.

Catalysts	Recycle times	Conv. (%)	Selectivity (%)					Iso-alkanes/*n*-alkanes (mol/mol)	C_{16}/C_{15} (mol/mol)
			n-C_{14}	iso-C_{15}	*n*-C_{15}	iso-C_{16}	*n*-C_{16}		
Co/HZ-1	1	> 99	1.2	22.3	9.6	51.1	15.8	2.8	2.1
	2	> 99	–	30.2	12.7	44.9	12.2	3.0	1.4
	3	> 99	–	26.2	18.0	43.9	11.9	2.3	1.3
	4	> 99	–	32.8	17.4	37.1	12.7	2.3	1.0
	5	> 99	–	32.4	22.3	34.6	10.7	2.0	0.8

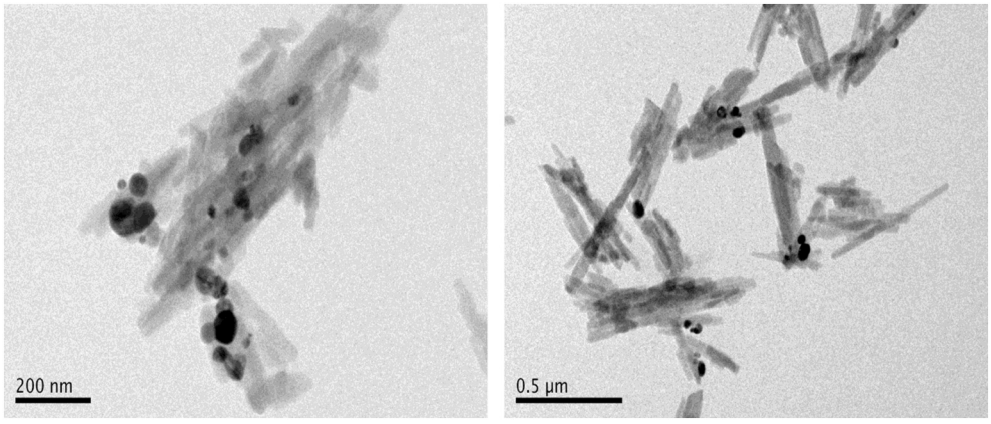

Fig. 6. TEM image of reduced Co/HZ-1 catalyst used after 5 cycles.

into H-ZSM-22 led to more weak and strong acid sites than the impregnation of Ni particles, especially for strong acid sites, which was beneficial for isomerization to produce more iso-products. Therefore, Co/H-ZSM-22 catalysts with low Co loading could be more appropriate bi-functional catalysts for upgrading of bio-oil to produce high quality jet fuel.

3.3.3. Influence of different reaction time

Catalytic performance over Co/HZ-1 catalyst in upgrading palmitic with different reaction time is shown in Table 4 at 260 °C for 2 MPa H_2. With complete conversion and deoxygenation of palmitic acid at 0.5 h, the selectivity of main products were 0.4% *n*-C_{14}, 12.1% iso-C_{15}, 16.8% *n*-C_{15}, 42.1% iso-C_{16} and 28.6% *n*-C_{16}, indicating that heating process for 1 h could improve the palmitic acid conversion. With prolonging reaction time, more *n*-C_{14} and iso-products were formed, and the molar ratio iso-alkanes/n-alkanes increased from 1.2 (0.5 h) to 2.8 (4 h). There was no obvious various C_{16}/C_{15} molar ratio at 0.5 h, 1 h, 2 h and 4 h for 2.2, 2.1, 2.1, and 2.1 respectively, proving that the deoxygenation routes did not change for long reaction time. That is, prolonging reaction time could increase the accessible opportunity between reactants and active centers of catalysts, leading to enhancing the iso-alkanses, rather than tailoring deoxygenation route.

3.3.4. Stability studies of bi-functional HZ-1 catalyst

Based upon its excellent catalytic performance during upgrading of palmitic acid, bi-functional Co/HZ-1 (incipient wetness impregnation

method) catalyst also evaluated the stability with the same catalytic experimental conditions (260 °C, 4 h, 2 MPa H_2) without internal/external mass transfer. The reusability of Co/HZ-1 (powered catalysts, five runs) are investigated. After each run, Co/HZ-1 was separated from the reaction mixture and dried at 105 °C for 10 min. As shown in Table 5, there was no deactivation occurred after five successive reactions with the identical condition, presenting excellent stability in catalytic performance. With increasing the recycles, main products (*n*-C_{16}, iso-C_{16}, *n*-C_{15}, and isoC_{15}) did not change; however, isoalkanes/*n*-alkanes and C_{16}/C_{15} both decreased from 2.8 (I) to 2.0 (V), from 2.1 (I) to 0.8 (V) respectively. The decrease of isoproducts might be relative to the coverage of acid sites in part, and the decrease of C_{16} might cause by the aggregation of metal particles. Fig. 6 gives TEM image of Co/HZ-1 with five runs, and it could be observed that some Co particles aggregated into large one, and more Co particles exposed over external surface of zeolites. These may be crucial factors to influence the stability of catalysts.

4. Conclusion

Bi-functional Co/HZ-1 and Co/HZ-2 catalysts were prepared by incipient wetness impregnation (3.9 wt% Co loading) and melt infiltration methods (3.7 wt% Co loading), respectively. Compared to parent HZ, the impregnation of Co into HZ could improve the acid strength regardless of some blockage micropores. Because of higher Co loading, Co/HZ-1 possessed more acid sites; otherwise, Co/HZ-2 had more serious blockage of micropores, disclosing that melt infiltration method might be beneficial for metal dispersion. Furthermore, simultaneous hydrodeoxygenation and hydroisomerization could be achieved over the bi-functional Co/H-ZSM-22 catalysts mainly via HDO route, and the maximum of iso-products could yield 73.4% selectivity. Co/H-ZSM-22 catalysts exhibited excellent catalytic performance with complete conversion of palmitic acid into 100% alkanes at low reaction H_2 pressure (1 MPa). Despite of the decrease of H_2 pressure, more C_{15} produced, indicating that low pressure favored HDC route. Due to the higher Co loading and more acid sites, Co/HZ-1 prepared by incipient wetness impregnation method yielded more C_{16} and iso-alkanes selectivity. Bi-functional Co/HZ-1 catalyst performed great stability of palmitic acid conversion. The aggregation and leaching of Co particles in recycle runs affected the product distribution to some extent.

Acknowledgements

The authors are grateful for the financial supports from Research Project of Guangdong Provincial Department of Science and Technology Department (No. 2015B020215004), the National Natural Science Foundation of China (No. 21576155, No. 21376140), and Program for Changjiang Scholars and Innovative Research Team in University (No. IRT13026), and research project supported by Airbus Group. Thank Ziyi Cui from Shangdong Experimental High School for her work in catalyst characterization and activity evaluation.

References

[1] J. Cheng, T. Li, R. Huang, J.H. Zhou, K.F. Cen, Optimizing catalysis conditions to decrease aromatic hydrocarbons and increase alkanes for improving jet biofuel quality, Bioresour. Technol. 158 (2014) 378–382.
[2] A. Srifa, N. Viriya-empikul, S. Assabumrungrat, K. Faungnawakij, Catalytic behaviors of Ni/γ-Al_2O_3 and Co/γ-Al_2O_3 during the hydrodeoxygenation of palm oil, Catal. Sci. Technol. 5 (2015) 3693–3705.
[3] D.C. Elliott, T.R. Hart, G.G. Neuenschwander, L.J. Rotness, G. Roesijadi, A.H. Zacher, J.K. Magnuson, Hydrothermal processing of macroalgal feedstocks in continuous-flow reactors, ACS Sustain. Chem. Eng. 2 (2) (2013) 207–215.
[4] M.P. Caporgno, E. Clavero, C. Torras, J. Salvadó, O. Lepine, J. Pruvost, J. Legrand, J. Giralt, C. Bengoa, Energy and nutrients recovery from lipid-extracted Nannochloropsis via anaerobic digestion and hydrothermal liquefaction, ACS Sustain. Chem. Eng. 4 (2016) 3133– – 3139.
[5] N. Shi, Q.Y. Liu, T. Jiang, T.J. Wang, L.L. Ma, Q. Zhang, X.H. Zhang, Hydrodeooxygenation of vegetable oils to liquid alkane fuels over Ni/HZSM-5 catalysts: methyl hexadecanoate as the model compound, Catal. Commun. 20 (2012) 80–84.
[6] H.L. Zuo, Q.Y. Liu, T.J. Wang, L.L. Ma, Q. Zhang, A. Zhang, Hydrodeoxygenation of methyl palmitate over supported Ni catalysts for diesel-like fuel production, Energy Fuel 26 (2012) 3747–3755.
[7] Q.Y. Liu, Y.W. Bie, S.B. Qiu, Q. Zhang, J. Sainio, T.J. Wang, L.L. Ma, J. Lehtonen, Hydrogenolysis of methyl heptanoate over co based catalysts: mediation of support property on activity and product distribution, Appl. Catal. B Environ. 147 (2014) 236–245.
[8] T.S. Nguyen, S. He, G. Raman, K. Seshan, Catalytic hydro-pyrolysis of lignocellulosic biomass over dual Na_2CO_3/Al_2O_3 and Pt/Al_2O_3 catalysts using n-butane at ambient pressure, Chem. Eng. J. 299 (2016) 415–419.
[9] H.L. Wang, H.X. Ben, H. Ruan, L.B. Zhang, Y.Q. Pu, M.Q. Feng, Arthur J. Ragauskas, B. Yang, Effects of lignin structure on hydrodeoxygenation reactivity of pinewood lignin to valuable chemicals, ACS Sustain. Chem. Eng. 5 (2017) 1824– – 1830.
[10] Q.Y. Liu, H.L. Zuo, T.J. Wang, L.L. Ma, Q. Zhang, One-step hydrodeoxygenation of palm oil to isomerized hydrocarbon fuels over Ni supported on nano-sized SAPO-11 catalysts, Appl. Catal. A Gen. 468 (2013) 68–74.
[11] A. Srifa, K. Faungnawakij, V. Itthibenchapong, N. Viriya-Empikul, T. Charinpanitkul, S. Assabumrungrat, Production of bio-hydrogenated diesel by catalytic hydrotreating of palm oil over $NiMoS_2/\gamma$-Al_2O_3 catalyst, Bioresour. Technol. 158 (2014) 81–90.
[12] Y. Xue, S. Zhou, X.L. Bai, Role of hydrogen transfer during catalytic copyrolysis of lignin and tetralin over HZSM-5 and HY zeolite catalysts, ACS Sustain. Chem. Eng. 4 (8) (2016) 4237–4250.
[13] R.R. Ding, Y.L. Wu, Y. Chen, J.M. Liang, J. Liu, M.D. Yang, Effective hydrodeoxygenation of palmitic acid to diesel-like hydrocarbons over MoO_2/CNTs catalyst, Chem. Eng. Sci. 135 (2015) 517–525.
[14] R.R. Ding, Y.L. Wu, Y. Chen, H. Chen, J.L. Wang, Y.C. Shi, M.D. Yang, Catalytic hydrodeoxygenation of palmitic acid over a bifunctional Co-doped MoO_2/CNTs catalyst: an insight into the promoting effect of cobalt, Catal. Sci. Technol. 6 (2016) 2065–2076.
[15] L. Ha, J. Mao, J. Zhou, Z.C. Zhang, S. Zhang, Skeletal isomerization of unsaturated fatty acids on beta zeolites: effects of calcination temperature and additives, Appl. Catal. A Gen. 356 (1) (2009) 52–56.
[16] B. Bozbiyik, J. Lannoeye, D.E. De Vos, G.V. Baron, J.F. Denayer, Shape selective properties of the Al-fumarate metal-organic framework in the adsorption and separation of n-alkanes, iso-alkanes, cyclo-alkanes and aromatic hydrocarbons, Phys. Chem. Chem. Phys. 18 (4) (2016) 3294–3301.
[17] B. Peng, X. Yuan, C. Zhao, J.A. Lercher, Stabilizing catalytic pathways via redundancy: selective reduction of microalgae oil to alkanes, J. Am. Chem. Soc. 134 (22) (2012) 9400–9405.
[18] B. Peng, Y. Yao, C. Zhao, J.A. Lercher, Towards quantitative conversion of microalgae oil to diesel-range alkanes with bifunctional catalysts, Angew. Chem. 124 (9) (2012) 2114–2117.
[19] B. Ma, C. Zhao, High-grade diesel production by hydrodeoxygenation of palm oil over a hierarchically structured Ni/HBEA catalyst, Green Chem. 17 (3) (2015) 1692–1701.
[20] Y.C. Shi, Y.Y. Cao, Y.N. Duan, H. Chen, Y. Chen, M.D. Yang, Y.L. Wu, Upgrading of palmitic acid to iso-alkanes over bi-functional Mo/ZSM-22 catalysts, Green Chem. 18 (2016) 4633–4848.
[21] Y.Y. Cao, Y.C. Shi, J.M. Liang, Y.L. Wu, S.B. Huang, J.L. Wang, M.D. Yang, H.S. Hu, High iso-alkanes production from palmitic acid over bi-functional Ni/H-ZSM-22 catalysts, Chem. Eng. Sci. 158 (2017) 188–195.
[22] T. Mochizuki, S.Y. Chen, M. Toba, Y. Yoshimura, Deoxygenation of guaiacol and woody tar over reduced catalysts, Appl. Catal. B Environ. 146 (2014) 237–243.
[23] K.K. Ramasamy, M. Gray, H. Job, Y. Wang, Direct syngas hydrogenation over a Co-Ni bimetallic catalyst: process parameter optimization, Chem. Eng. Sci. 135 (2015) 266–273.
[24] D. Sahoo, S. Vajpai, S. Patel, K.K. Pant, Kinetic modeling of steam reforming of ethanol for the production of hydrogen over Co/Al_2O_3 catalyst, Chem. Eng. J. 125 (3) (2007) 139–147.
[25] T.M. Huynh, U. Armbruster, M.M. Pohl, M. Schneider, J. Radnik, D.L. Hoang, B.M. Quoc Phan, D.A. Nguyen, A. Martin, Hydrodeoxygenation of phenol as a model compound for bio-oil on non-noble bimetallic nickel-based catalysts, ChemCatChem 6 (7) (2014) 1940–1951.
[26] J. Majewska, B. Michalkiewicz, Production of hydrogen and carbon nanomaterials from methane using Co/ZSM-5 catalyst, Int. J. Hydrog. Energy 41 (20) (2016) 8668–8678.
[27] F. Lónyi, H.E. Solt, Z. Pászti, J. Valyon, Mechanism of NO-SCR by methane over co, H-ZSM-5 and Co, H-mordenite catalysts, Appl. Catal. B Environ. 150 (2014) 218–229.
[28] Y. Yan, L. Wang, H.P. Zhang, Catalytic combustion of volatile organic compounds over Co/ZSM-5 coated on stainless steel fibers, Chem. Eng. J. 255 (2014) 195–204.
[29] Y. Ono, Y. Fujii, H. Wakita, K. Kimura, T. Inui, Catalytic combustion of odors in domestic spaces on ion-exchanged zeolites, Appl. Catal. B Environ. 16 (3) (1998) 227–233.
[30] G. Vitale, H. Molero, E. Hernandez, S. Aquino, V. Birss, P. Pereira-Almao, One-pot preparation and characterization of bifunctional Ni-containing ZSM-5 catalysts, Appl. Catal. A Gen. 452 (2013) 75–87.
[31] S. Wong, N. Ngadi, T.A. Tuan Abdullah, I.M. Inuwa, Catalytic cracking of LDPE dissolved in benzene using nickel-impregnated zeolites, Ind. Eng. Chem. Res. 55 (9) (2016) 2543–2555.